

URTeC: 4031314

## Field Implementation and Surveillance of Gas Injection Enhanced Oil Recovery in the Bakken

Jin Zhao, Lu Jin\*, Xue Yu, Nicholas A. Azzolina, Xincheng Wan, Steven A. Smith, Nicholas W. Bosshart, James A. Sorensen. Energy & Environmental Research Center, University of North Dakota.

Copyright 2024, Unconventional Resources Technology Conference (URTeC) DOI 10.15530/urtec-2024-4031314

This paper was prepared for presentation at the Unconventional Resources Technology Conference held in Houston, Texas, USA, 17-19 June 2024.

The URTeC Technical Program Committee accepted this presentation on the basis of information contained in an abstract submitted by the author(s). The contents of this paper have not been reviewed by URTeC and URTeC does not warrant the accuracy, reliability, or timeliness of any information herein. All information is the responsibility of, and, is subject to corrections by the author(s). Any person or entity that relies on any information obtained from this paper does so at their own risk. The information herein does not necessarily reflect any position of URTeC. Any reproduction, distribution, or storage of any part of this paper by anyone other than the author without the written consent of URTeC is prohibited.

---

### Abstract

Various laboratory and modeling activities have been performed to offset the rapid oil production decline in single wells to investigate enhanced oil recovery (EOR) in unconventional reservoirs. Several field pilots have also been conducted to test the EOR effects of different methods in major unconventional plays. Although high oil recovery was reported in laboratory and modeling work, the EOR results in field pilots were mixed. To fill the gap between theoretical work and field implementations, case studies were evaluated in this work to analyze the actual gas injection EOR field tests in the Bakken petroleum system (BPS). Based on these pilots, an EOR-monitoring workflow was developed to explore real-time visualization, forecasting, and control methods for improved reservoir surveillance during EOR processes.

Eleven EOR pilot studies that used rich gas, CO<sub>2</sub>, surfactant, water, or their combinations have been conducted in the BPS since 2008. Gas injection was involved in eight of these pilots with huff 'n' puff, flooding, and injectivity operations. Surveillance data, including daily production/injection rates, bottomhole injection pressure, gas composition, and tracer testing, were collected from these tests to generate time-series plots or analytics that can inform operators of downhole conditions. Predictive modeling based on reservoir simulation and machine learning was then conducted to rapidly forecast future performance for operators to compare against observed performance. The real-time comparison enables operators to take control actions to improve EOR outcome.

Case studies showed that pressure buildup, conformance issues, and timely gas breakthrough detection were some of the main challenges because of the interconnected fractures between injection and offset wells. The latest operation of coinjecting gas, water, and surfactant through the same injection well showed that these challenges could be mitigated by careful EOR design and continuous reservoir monitoring. A user interface was developed to integrate EOR-monitoring components and provide real-time visualization to enable operators to modify key EOR parameters, such as gas injection rate and pressure, and rapidly predict the subsequent EOR outcome. Results showed that monitoring gas composition could be more sensitive for detecting premature gas breakthroughs than other indicators.

Since only limited research has been reported to investigate actual field implementations and their surveillance, the findings in this study provided the necessary technical support to demonstrate how injecting gas into a Bakken reservoir can be used for EOR, thereby increasing ultimate oil recovery while reducing produced gas flaring and greenhouse gas emissions. With an increasing number of wells entering their late phase with low or uneconomical oil production rates, it is anticipated that the scientific understanding gained from field implementation and surveillance activities will lead to commercial deployment of gas injection EOR in the BPS and other unconventional plays within the next decade and perhaps sooner.

## Introduction

Enhanced oil recovery (EOR) technologies have been used to restore oil production in conventional reservoirs for decades. To offset the rapid single-well oil production rate and reproduce the success of EOR in unconventional reservoirs, many experimental, modeling, and simulation studies have been performed to understand the fundamental oil recovery mechanisms in these formations with ultralow permeability [1–7]. In addition, a few pilot tests have been conducted in some of the main unconventional oil plays, including the Bakken petroleum system (BPS), Eagle Ford, and Permian Basin, to examine EOR performance in actual fields. The pilots in the BPS showed that gas injection was the most popular EOR method, and injectivity was not an issue because of the highly connected fractures between wells [8–15]. However, this good connectivity also caused a significant challenge for gas containment (i.e., gas injected into one well rapidly migrated to other wells or unknown regions in the formation) [9, 16–18]. As a result, pressure could not build up around the EOR wells for gas to penetrate and extract oil from the tight rocks. Therefore, monitoring gas breakthrough behavior in offset wells has become a key factor for operators to control an EOR process.

Various monitoring technologies have been used to detect fluid breakthrough behavior in conventional reservoirs when waterflooding or gasflooding operations are implemented [19–23]. For example, pulsed-neutron logs and seismic surveys are frequently used to detect whether gas has entered a production well or passed a certain location in a CO<sub>2</sub>-flooding process [22–27]. However, such methods usually require days to weeks to interpret the measured data (i.e., these methods do not produce near-real-time data/information). In addition, EOR implemented in conventional reservoirs typically utilizes vertical wells arranged in flood patterns instead of unconventional Bakken reservoir development, which utilizes long horizontal wells (laterals) with 10,000 ft or more of completed lateral. Using conventional production logs, it is challenging to evaluate the flow behavior in long horizontal wells with tens of fracture stages. The complex completion methods for unconventional reservoirs, like the Bakken, combined with reservoir heterogeneity make regular production data (oil/gas/water rates) too noisy to detect gas breakthrough accurately [28].

Tracer testing has been used in the oil and gas industry for many years with a range of applications, including evaluation of reservoir heterogeneity, determination of connectivity between wells/fractures, identification of thief zones (as well as flow barriers) in a reservoir, and estimation of sweep efficiency [29–32]. The fast evolution of tracer technologies has made tracer testing an important monitoring and surveillance method for field practices, including various EOR operations [33, 34]. Various tracers have been developed in the past decades, and different tracers can be used to rapidly identify and characterize the movement of gas, oil, or water, depending on the project requirements [35–37].

Since interwell connectivity is common between hydraulically fractured wells, the goals of this study were to 1) study well interference effects on actual gas injection EOR performance in the Bakken Formation and 2) explore real-time visualization, forecasting, and control methods for improved reservoir surveillance during gas injection EOR. The integration of these pieces—visualizing reservoir surveillance data in real-time and rapidly forecasting reservoir performance—constitutes the workflow for gas EOR monitoring in unconventional reservoirs.

## Review of EOR Surveillance in the BPS

This section presents a review of reservoir surveillance data generated for previous Bakken EOR pilot tests, which used rich gas, carbon dioxide, surfactant, water, or combinations of these fluids. The operational data were used to screen candidate effective EOR-monitoring methods, which were then applied to an extensive set of reservoir simulation outputs of a reference gas EOR project to evaluate gas breakthrough at offset production wells.

### Overview of EOR Pilot Tests

**Table 1** provides general information for the previous pilots, including pilot test time, injectate, operational method, operator/reporter, and state and county (if available). Ten pilot tests were conducted in North Dakota, and two were conducted in Montana [16].

Table 1. Summary of Bakken EOR Pilot Tests Used to Screen Candidate EOR-Monitoring Methods

Case No.	Pilot Start Year	Injectate	Operational Method	Operator/Reporter	State/County
1	1994	Water	HnP <sup>1</sup>	Meridian	ND/McKenzie
2	2012	Water	HnP	EOG	ND/Mountrail
3	2014	Water	Flooding	Montana Tech	MT/(county N/A <sup>2</sup> )
4	2015	Surfactant	HnP	Nalco Champion	ND/(county N/A)
5	2008	CO <sub>2</sub>	HnP	EOG	ND/Mountrail
6	2009	CO <sub>2</sub>	HnP	Continental	MT/(county N/A)
7	2014	CO <sub>2</sub>	Flooding/injectivity	Whiting	ND/Mountrail
8	2017	CO <sub>2</sub>	Injectivity	XTO	ND/Dunn
9	2017	Propane	Flooding	Hess	ND/Mountrail
10	2014	Rich gas	Flooding	EOG	ND/Mountrail
11	2018	Rich gas	HnP	Liberty	ND/Williams
12	2021	Rich gas, water, surfactant	HnP	Liberty	ND/Mountrail

1: Huff 'n' puff, an operational method for EOR.

2: Not available.

While many different technologies have been developed and applied to monitor the EOR process in conventional reservoirs, comparatively fewer technologies were used in the historical Bakken EOR pilot tests to monitor injection and production behavior. As shown in **Table 2**, most of the Bakken EOR pilot studies included monthly production and/or injection rates (oil, gas, and water volumes per month) and well logs. Six pilots had daily production/injection rates, and four pilots had bottomhole pressure (BHP) measurements. Three pilots included gas composition monitoring, and two pilots had tracer testing. The table shows that eight of the pilot tests employed gas injection (propane, rich gas, or CO<sub>2</sub>), and three successful cases (Case Nos. 8, 9, and 12) were reported with a gas injectate (hereafter, gas EOR) involved. Relatively comprehensive monitoring data were generated in Cases 9, 11, and 12 to analyze Bakken gas EOR processes [28].

### Case Study 1: Rich Gas HnP

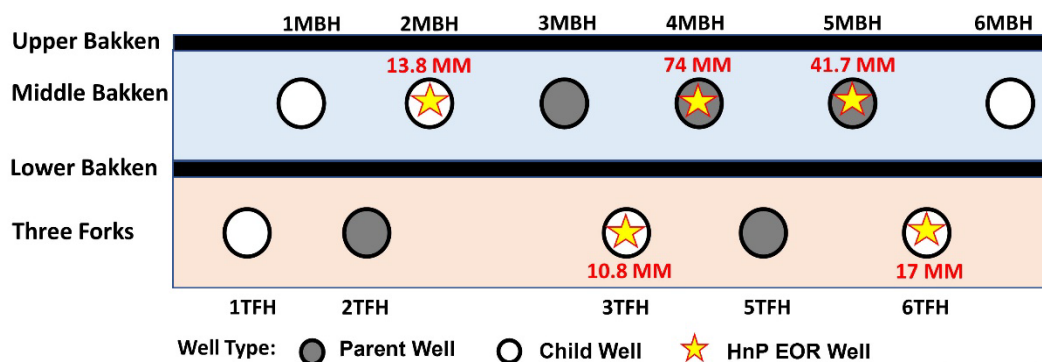
A cyclic multiwell HnP EOR pilot (Case No. 11) using rich gas was performed by Liberty Resources LLC (Liberty) in Williams County, North Dakota, from July 2018 through May 2019 [11]. Eleven horizontal wells were drilled and completed in the drilling space unit (DSU), and five of them were used for HnP operations, as illustrated in **Figure 1**. A total of ~160 MMscf of rich gas was injected into the formation through these wells. An extensive monitoring dataset, including daily production and injection rates, BHP, gas composition, and tracer testing data, was generated during the pilot period. **Figure 2** shows the change of BHP with cumulative gas injection in the EOR wells.

Table 2. Summary of Available Data for the Previous Bakken EOR Pilot Tests

Case No.	Injectate	Routine Data	Monitoring Methods/ Data Reported	Data Source
1	Water	MPIR, <sup>1</sup> well logs		[38]
2	Water	MPIR, well logs		[38]
3	Water	MPIR	Daily injection rate	[9, 38]
4	Surfactant	MPIR		[8]
5	CO <sub>2</sub>	MPIR, well logs		[38]
6	CO <sub>2</sub>	MPIR		[9]
7	CO <sub>2</sub>	MPIR, well logs	Daily injection rate, WHP <sup>2</sup> , gas composition	[38]
8	CO <sub>2</sub>	MPIR, well logs	Daily injection rate, BHP, oil composition	[10, 38]
9	Propane	MPIR, well logs	Daily production/injection rates, WHP, gas composition, tracer testing	[14, 38]
10	Rich gas	MPIR, well logs		[38]
11	Rich gas	MPIR, well logs	Daily production/injection rates, BHP, gas composition, tracer testing	[11, 38]
12	Rich gas, water, surfactant	MPIR, well logs	Minutely and daily production/injection rates, WHP, BHP	[12, 38]

1: Monthly production and injection rates.

2: Wellhead pressure.



EERC LJ65296.PSD

Figure 1. Cross section of well distribution at the Liberty rich gas EOR site (Case 11), where five wells were used for HnP operations in the field.

Generally, BHP increased initially with gas injection and then leveled off after injecting ~13 MMscf of rich gas in most wells. None of the wells reached minimum miscibility pressure (MMP) between the oil and rich gas (~2500 psi) under reservoir conditions.

The BHP behavior demonstrated that the injected gas filled the fractures and then rapidly migrated to the produced volume around the wells. The tracer analysis confirmed this inference: gas tracer breakthrough was observed in offset wells within 48 hours, often followed by increased gas-to-oil ratio (GOR) [11]. The gas production in the puff stages showed that around 91% of the injected gas could be recovered from both the HnP and offset wells. This observation indicated that most of the injected gas migrated to offset wells through fractures instead of building BHP, penetrating the tight rocks, and extracting oil from there in the EOR process.

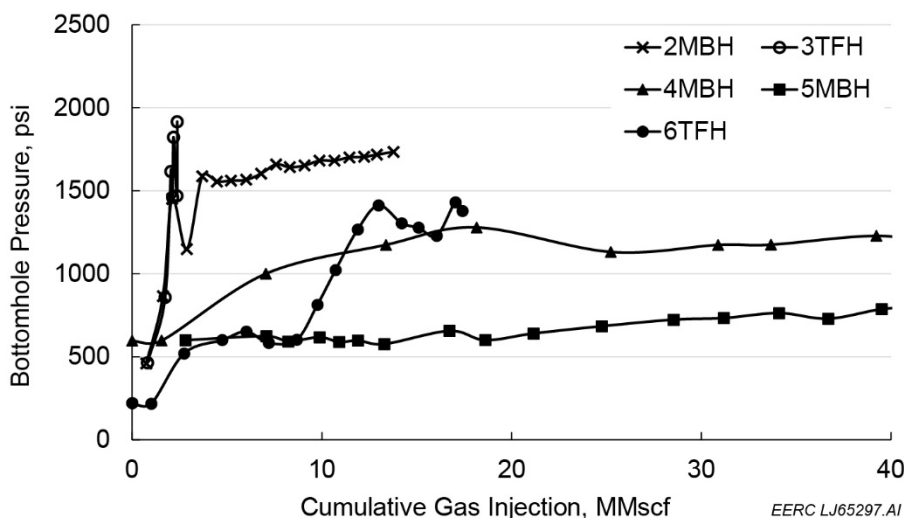


Figure 2. BHP changes with cumulative gas injection in the rich gas EOR process.

### Case Study 2: Propane Flooding

**Figure 3** illustrates the distribution of the gas injection well and its offset production wells in the propane EOR pilot test (Case No. 9) conducted in the BPS by Hess Corporation from May 2017 through November 2018. A vertical well, C3\_Inj, was used to inject propane, and oil/gas/water production rates were monitored at the offset production wells, M1–M6, which were connected to horizontal laterals of different lengths. Well M1 was the closest production well to the propane injection well, with a distance of around 1000 ft. Compared to massive fracture connectivity in other cases, the fracture connectivity between C3\_Inj and M1 was limited in this case. A total of 19.88 MMscf of propane was intermittently injected into C3\_Inj from May 2017 through August 2018. The injection rate varied from month to month, as shown in **Figure 4**. The WHP was maintained between 4200 and 4500 psi, which was much greater than the first miscibility pressure (650 psi) between propane and oil under reservoir temperature (220°F). Similar to other cases, no injectivity problem was experienced during the injection process except for some injection interruptions caused by mechanical issues [14–15].

**Figure 5** shows the daily fluid production rates (gas, oil, and water) for M1 and the propane injection rate for C3-Inj. As shown in the figure, the fluid production rates do not provide sufficient information to determine if and/or when the injected propane breakthrough occurred in the offset production well, M1. In contrast, compositional measurements of the gas stream produced from M1 provided robust signals for gas breakthrough diagnosis. The propane concentration (in mole percentage) in the produced gas stream from a normal Bakken production well is usually below 20 mol% based on many pressure, volume, and temperature reports collected from the BPS. This concentration can be relatively stable for a long time during the normal production process. Accordingly, a propane concentration in the produced gas stream of an offset well that is significantly higher than 20 mol% could be a clear signal of propane breakthrough.

**Figure 6** demonstrates how the propane concentration changed in the produced gas stream of M1 during the monitoring period. The data showed that the propane concentration exceeded 93 mol% on October 10, 2017, which clearly indicated that the injected propane had breakthrough to the M1 well as most of the produced gas was propane. Since 19.88 MMscf of propane was injected into the formation near M1, the propane production from this well lasted for months after injection operations ceased in C3\_Inj. The prolonged high-concentration propane production in M1 also showed that the injected gas could be contained in the target reservoir volume for a long time when the EOR wells were selected properly (e.g., limited connectivity between wells).

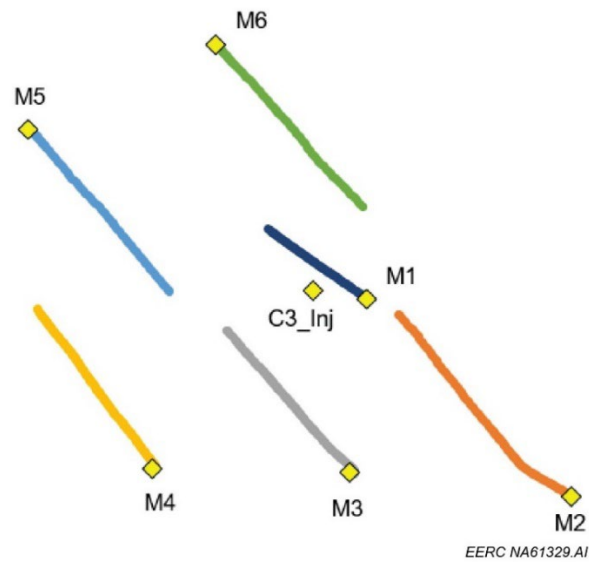


Figure 3. Schematic of the gas injection well (C3\_Inj), offset production wells (M1–M6), and horizontal laterals in the Hess propane EOR pilot test.

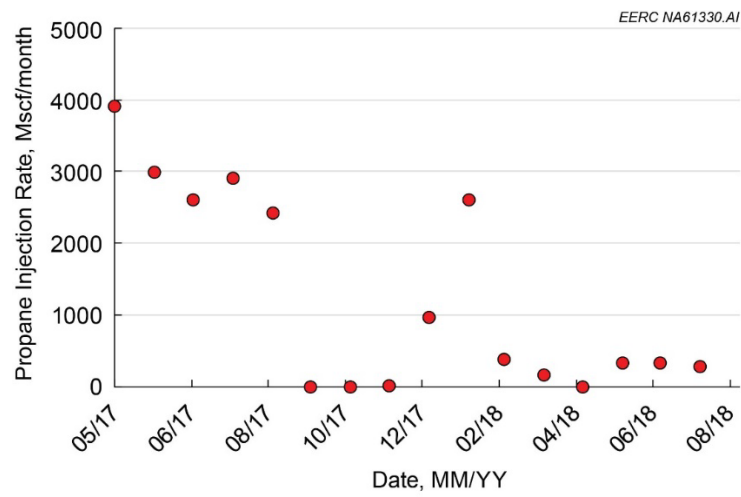


Figure 4. Monthly gas injection rate in the Hess propane EOR pilot test.



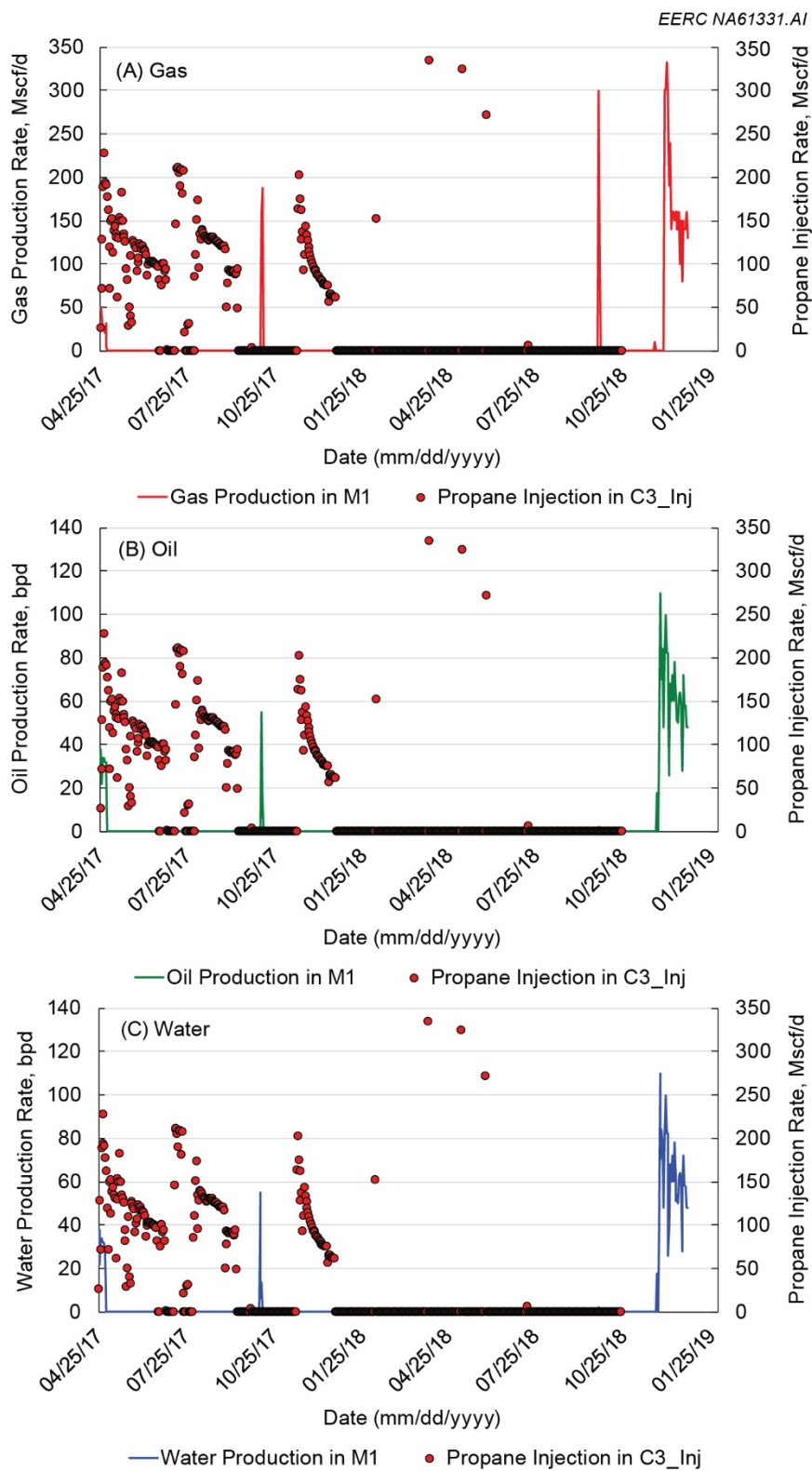


Figure 5. Daily fluid production rate and propane injection rate in M1 and C3\_Inj, respectively, and for the Hess propane EOR pilot test: A, gas; B, oil; and C, water.

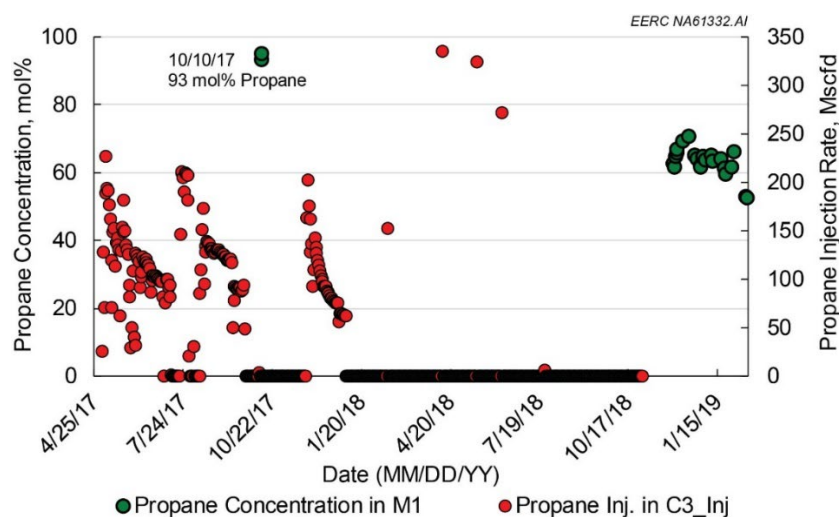


Figure 6. Monitoring of propane concentration in the gas stream produced from M1 (mol%, left y-axis) and propane injection rate in C3\_Inj (right y-axis) for the Hess propane EOR pilot test.

### Case Study 3: Rich Gas–Water–Surfactant HnP

In 2021, Liberty performed a single-well HnP pilot (Case No. 12) using rich gas, water, and surfactant in a 2560-acre DSU in Mountrail County, North Dakota [12]. Based on experience from the previous rich gas HnP pilot (Case No. 11), this pilot was specifically designed to 1) build BHP to inject gas at low surface pressures and improve gas conformance in the reservoir, 2) repressure the reservoir above MMP around the HnP well, and 3) use a surfactant to improve EOR performance through changing rock wettability and reducing interfacial tension between the reservoir fluids and the injected EOR agents.

Figure 7 illustrates the arrangement of wells for the pilot test: the middle well (10MBH) was selected for HnP operations, two offset wells (1TFH and 4TFH) were used as the main monitoring wells, and the remaining four wells (1MBH, 2TFH, 3MBH, and 4MBH) were used as monitoring and boundary wells. The monitoring wells were produced continuously during the pilot to limit possible migration of the injected fluids out of the DSU. A supervisory control and data acquisition system was employed to collect high-frequency rate and pressure data in the HnP well. The pilot test was performed with one cycle of injection from September 10, 2021, through October 11, 2021, followed by regular production operations. A total of 46 MMscf of gas, 40,000 bbl of water, and 2400 gallons of surfactant were injected into the HnP well during the injection cycle.

A new injection technology called the rapid-switched, stacked-slug (RSSS) system was utilized to perform water–gas coinjection. The technology could boost BHP to the desired level effectively while considerably reducing the requirement of surface injection pressure. This was a significant advantage for EOR

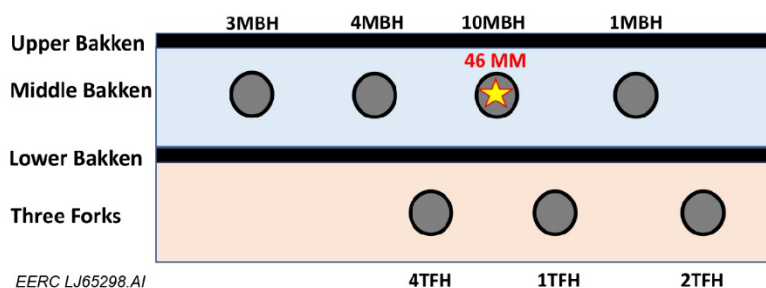


Figure 7. Cross section of well distribution for rich gas–water–surfactant EOR at the East Nesson site (Case No. 12), where one well was used for HnP operations in the field.



applications in fractured reservoirs compared to traditional gas compression along with the addition of surfactant. **Figure 8** shows gas and water injection rates at 10MBH during the injection cycle. The gas injection rate was relatively stable in the first 2 weeks and then decreased gradually. The water injection rate showed a different trend, gradually increasing in the first 2 weeks and then stabilizing. WHP and BHP response is illustrated in **Figure 9**. The injection increased BHP from 1000 to 4500 psi, while WHP maintained at around 1000 psi. This clearly demonstrated the effectiveness of the RSSS system for raising BHP without requiring high WHP during the injection process.

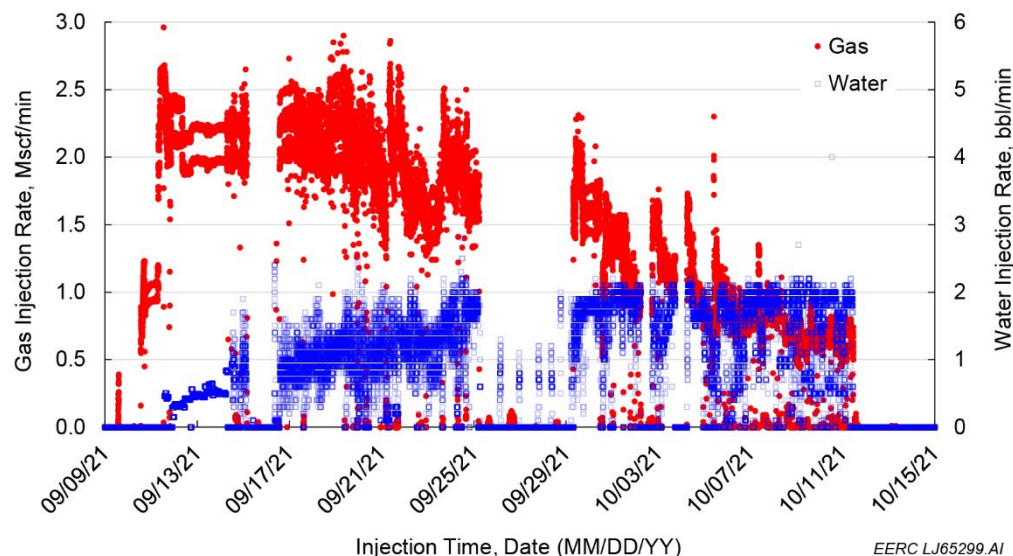


Figure 8. Gas and water injection rates at 10MBH during the injection cycle.

Gas and water production rates were closely monitored in the offset wells to observe the breakthrough of injected fluids into these wells. Once gas breakthrough was detected in an offset well, the RSSS system could rapidly adjust the water-to-gas ratio (WGR) in the HnP well to prevent large gas production increases in the offset wells. The high WGR greatly reduced the mobility of the injected fluids in the fractures so that the injected gas could be contained in the near-injection well area instead of flowing through the fractures and produced through the offset wells, as observed in Case No. 11. **Figure 10** shows the gas and water production rates in 1TFH in the HnP process. A minor gas breakthrough was observed in the well, but the conformance issue was effectively controlled by increasing the WGR in the HnP well. This observation indicated the potential of the RSSS technology to solve the conformance control issue, which is one of the most critical challenges for EOR in unconventional reservoirs.

### Simulation Model for EOR Monitoring

Premature gas breakthrough and poor conformance control have been identified as two of the most critical factors for underperforming gas EOR tests in the BPS, which was illustrated in Case No. 11. Case No. 12 showed that these issues could be mitigated by closely monitoring injection and production behavior in the EOR process and acting quickly after the detection of gas breakthrough. For gas EOR without water injection, tracer and/or injection gas composition analysis could efficiently detect premature gas breakthrough in offset wells, as demonstrated in Case Nos. 9 and 11. Therefore, reservoir simulations were performed in this study to investigate gas EOR monitoring in a Bakken DSU.

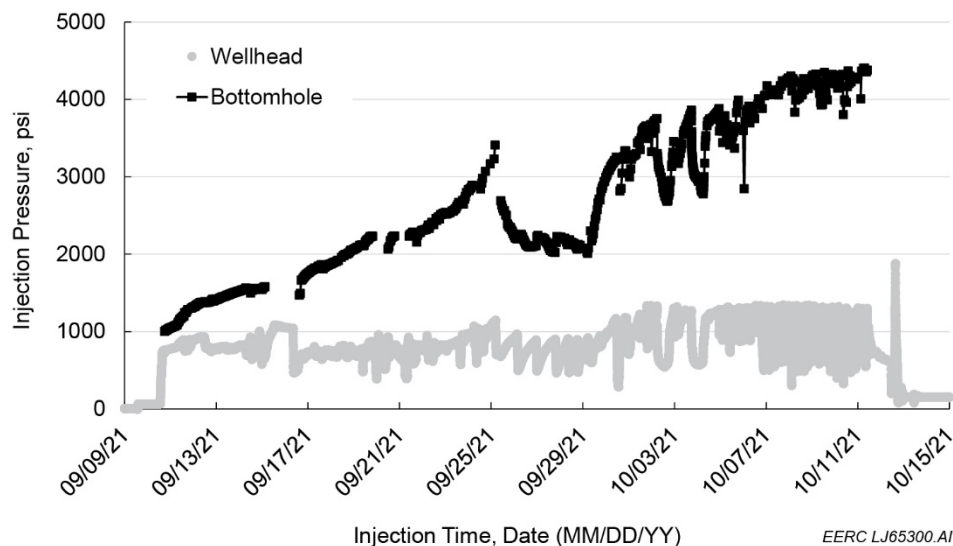


Figure 9. WHP and BHP at 10MBH during the injection cycle.

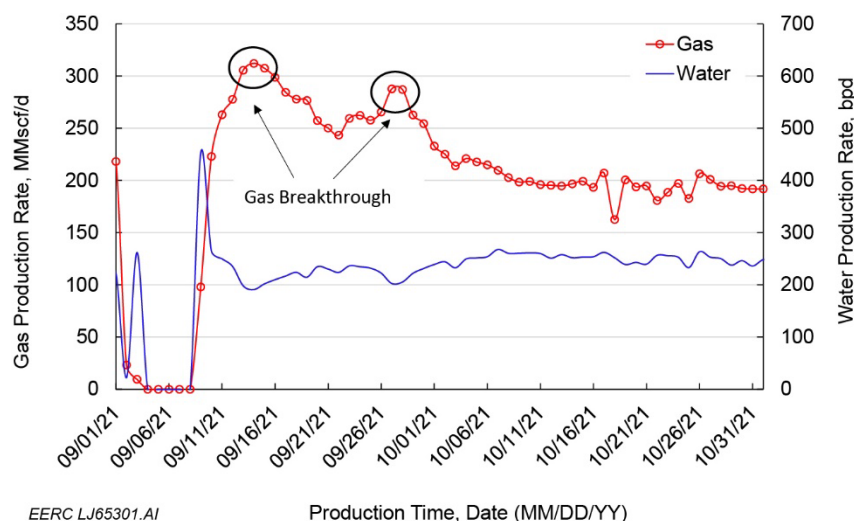


Figure 10. Monitoring of gas and water production rates in Offset Well 1TFH.

### Baseline Model of a Seven-Well DSU

A simulation model with seven wells in Dunn County, North Dakota, was adopted for EOR-monitoring simulation based on reported well interference and conformance control work [39, 40]. Three wells were completed in the Middle Bakken (MB) unit (MB1, MB2, and MB3), and four wells were completed in the Three Forks (TF) Formation (TF1, TF2, TF3, and TF4). Well interference was observed in the DSU, indicating the wells could be interconnected through fractures, as illustrated in [Figure 11](#). Using the geologic/reservoir properties, equation-of-state (EOS), and embedded discrete fracture model (EDFM) method, a compositional reservoir simulation model with main hydraulic fractures was developed to simulate gas EOR performance in this DSU employing Computer Modelling Group Ltd.'s (CMG's) GEM compositional simulation module.

The length (x direction), width (y direction), and height (z direction) of the simulation model are 4000, 3250, and 206 ft, respectively. The model was divided into five formations with a total of 17 layers, including the Lodgepole (LP), Upper Bakken (UB), MB, Lower Bakken (LB), and TF units, from the top to the bottom of the model. The thicknesses of the LP, UB, MB, LB, and TF are 40, 18, 40, 18, and 90 ft,

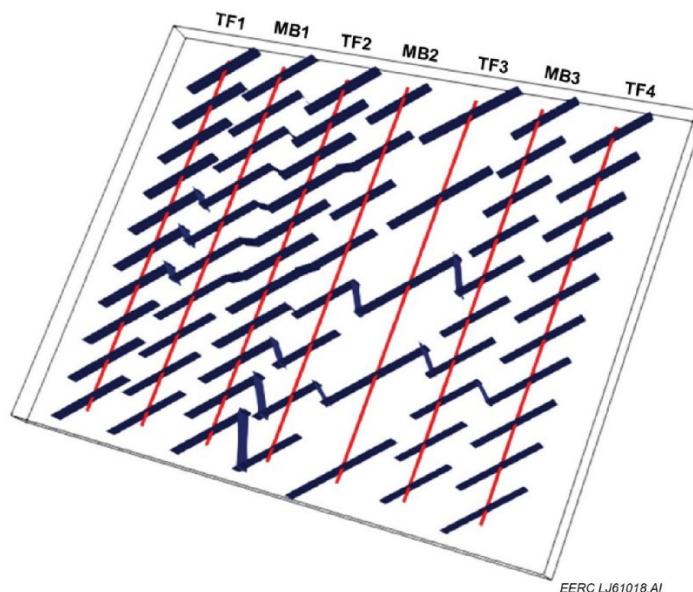


Figure 11. Schematic of fracture distribution in the simulation model for the Dunn site.

respectively. An additional 16 cells in the x direction were added to the EDFM for fracture calculation based on the algorithm described above. The additional cells were used for flow calculation only, and they did not change the material balance in the model. History matching was conducted to reproduce the production data in the DSU. The results indicated that the model was able to capture the production behavior of the wells within an acceptable margin of error.

### ***EOR Simulation***

**Figure 12** illustrates an example of well arrangement for gas EOR simulation using the history-matched model. The reservoir simulations evaluated scenarios with all wells open (i.e., Offset Wells MB1, MB3, TF1, TF2, TF3, and TF4 open) and scenarios with the exterior offset wells closed (i.e., Offset Wells MB1, MB3, TF1, and TF4 shut in and TF2 and TF3 open), as shown by the dashed and solid outlines in the figure. The yellow arrows in the figure illustrate potential gas flow paths from the injection well (MB2) to the offset production wells.

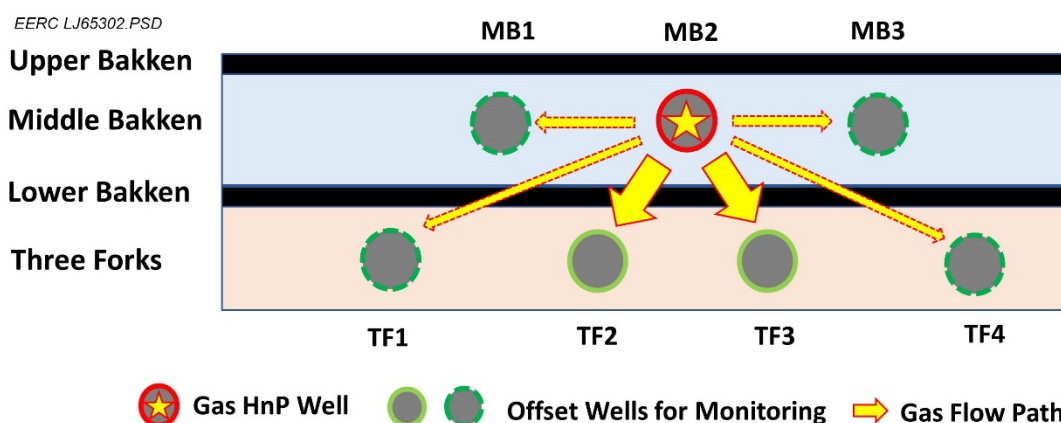


Figure 12. Illustration of an example well arrangement for gas EOR simulation using the seven-well DSU model.

One of the objectives for EOR monitoring was to rapidly detect gas breakthrough into the offset wells during the gas injection process. As summarized in the case study section, propane concentration could be used to detect gas breakthrough behavior more effectively than fluid production rates (oil, gas, or water).

Based on the same logic, if another pure gas like methane or ethane is injected for EOR operations, then its concentration could also be used to detect gas breakthrough. Therefore, the gas components were set up individually in the EOS so that pure-component gas injection scenarios could be simulated for methane, ethane, and propane.

In unconventional reservoirs, a short tracer breakthrough time in an offset well may indicate that fractures connect the well to the injection well. For example, the tracer tests in Case No. 11 showed that the wells were highly interconnected through fractures in the reservoir [11]. Therefore, tracer tests were included in the reservoir simulations for rich gas EOR to evaluate how the addition of a tracer gas would improve EOR monitoring as compared to rich gas or single-component gas injection without a tracer. Based on the rich gas composition (60 mol% of methane, 25 mol% of ethane, and 15 mol% of propane) simulated in this study, three tracers were attached to three individual gas components, as shown in Table 3: Tracers TRC-C1, TRC-C2, and TRC-C3 were attached to methane, ethane, and propane, respectively. Both pure propane and rich gas (with tracers) EOR scenarios were simulated using CMG's GEM 2020 version.

Table 3. Composition of the EOS for Gas Breakthrough and EOR Simulations

No.	Component	Tracer Attached	No.	Component	Tracer Attached
1	N <sub>2</sub>	N/A	5	IC <sub>4</sub> to NC <sub>4</sub>	N/A
2	CH <sub>4</sub>	TRC-C1	6	IC <sub>5</sub> to C <sub>12</sub>	N/A
3	C <sub>2</sub> H <sub>6</sub>	TRC-C2	7	C <sub>13</sub> to C <sub>19</sub>	N/A
4	C <sub>3</sub> H <sub>8</sub>	TRC-C3	8	C <sub>20</sub> to C <sub>30</sub>	N/A

Two sets of simulation cases were performed for the seven-well DSU: propane injection and rich gas injection with a tracer (hereafter, tracer injection). These sets were used to evaluate gas breakthrough from the gas injection well (MB2) to the offset production wells (MB1, MB3, and TF1–4) under different operating conditions, as shown in Table 4. Fifty-six simulations were performed for propane injection. The first 28 runs were executed with Offset Wells MB1, MB3, TF1, and TF4 closed (shut in) and with the wells open (producing) for the next 28 cases. The same settings were applied to tracer injection. Gas was injected at Well MB2 and utilized varying injection rates from 0.5 to 18 MMscfd and maximum injection BHP varying from 1500 to 7500 psi across the simulation runs. The rate and pressure settings were designed to cover representative operational ranges for the unconventional Bakken reservoir. The minimum production BHP (100 psi), injection time (30 days), soaking time (7 days), production time (60 days), and cycle time (97 days) were held constant across all runs. The injection–soaking–production cycles through 2 years of prediction can be found in Table 5.

Table 4. Reservoir Simulation Case Matrix for EOR Monitoring During the Propane and Tracer Injection Processes

Simulation Case No.	Indicator	TF2 and TF3 During Injection	MB1, MB3, TF1, and TF4 During Injection	Inj. Rate, MMscfd	Max. Inj. BHP, psi
1–28	Propane	Shut in	Shut in	0.5–18	1500–7500
29–56	Propane	Shut in	Open	0.5–18	1500–7500
57–84	Tracer	Shut in	Shut in	0.5–18	1500–7500
85–112	Tracer	Shut in	Open	0.5–18	1500–7500

Table 5. Injection–Soaking–Production Cycles in the HnP Process

Date (MM/DD/YY)	Cycle							
	1	2	3	4	5	6	7	8
<b>Injection Start</b>	01/01/20	04/07/20	07/13/20	10/18/20	01/23/21	04/30/21	08/05/21	11/10/21
<b>Injection End</b>	01/30/20	05/06/20	08/11/20	11/16/20	02/21/21	05/29/21	09/03/21	12/09/21
<b>Soaking Start</b>	01/31/20	05/07/20	08/12/20	11/17/20	02/22/21	05/30/21	09/04/21	12/10/21
<b>Soaking End</b>	02/06/20	05/13/20	08/18/20	11/23/20	02/28/21	06/05/21	09/10/21	12/16/21
<b>Production Start</b>	02/07/20	05/14/20	08/19/20	11/24/20	03/01/21	06/06/21	09/11/21	12/17/21
<b>Production End</b>	04/06/20	07/12/20	10/17/20	01/22/21	04/29/21	08/04/21	11/09/21	12/31/21

The wells were operated differently in the offset well open and closed scenarios. For cases with offset wells open, Wells MB1, MB3, TF1, TF2, TF3, and TF4 were open all the time (producing), and only Well MB2 changed its status with cycles, as shown in Table 6. For cases with offset wells closed, Wells TF1, MB1, MB3, and TF4 were closed all the time (shut in), and other wells changed their status with HnP stages, as shown in Table 7. These 112 cases were simulated to create input data for the machine learning (ML) and EOR-monitoring study.

Table 6. Change of Well Status for MB2 in Different HnP Stages When All of the Offset Wells (MB1, MB3, TF1, TF2, TF3, and TF4) Were Kept Open (producing)

Stage	Cycle 1 as an Example	Well Status	
	Date (MM/DD/YY)	Open	Closed
Injection	01/01/20 to 01/30/20	MB2 (injecting)	
Soaking	01/31/20 to 02/06/20		MB2
Producing	02/07/20 to 04/06/20	MB2	

Table 7. Change of Well Status for MB2, TF2, and TF3 in Different HnP Stages When External Offset Wells (MB1, MB2, TF1, TF2, TF3, and TF4) Were Closed (shut in)

Stage	Cycle 1 as an Example	Well Status	
	Date (MM/DD/YY)	Open	Closed
Injection	01/01/20 to 01/30/20	MB2 (injecting)	TF2, TF3
Soaking	01/31/20 to 02/06/20		TF2, MB2, TF3
Producing	02/07/20 to 04/06/20	TF2, MB2, TF3	

### Real-Time Visualization and Forecasting

Visualization refers to time-series plots of reservoir surveillance data or analytics (reexpressions of the data that provide better insights than the raw measurement) that can inform the EOR site operator of downhole conditions (e.g., gas breakthrough from the injection well[s] to the offset production well[s]) that could affect the performance of the EOR project. In this proof of concept, real-time visualization allows the user to display the simulation results for selected EOR operating parameters and target variables. The visualization process is meant to emulate real-time data that are consistent with similar processes that were applied to gas injection projects. For example, a typical field project for rich gas EOR might include the following sequence of steps: 1) acquiring injection rates, production rates, and well BHPs whenever new data are available, providing the foundation of real-time visualization;



2) preprocessing data to deal with missing and outlier values; 3) compiling the various datasets into a coherent structured data format based on well identifiers, operating scheme, and acquisition time stamp; 4) appending new data to the existing dataset; and 5) creating visualizations and/or updating visualizations based on the updated dataset.

In this proof-of-concept study, the process started with the data already acquired, transferred, aggregated, and cleaned, and the full 2-year EOR outputs were used in the visualizations. However, the process may be adapted to real time and can upload and plot the data at whatever acquisition frequency the field operator would like to implement (e.g., hourly, daily, weekly, etc.). The EOR operating parameters for the reservoir simulations included external offset well status (MB1, MB3, TF1, and TF4 closed or open), injectate (rich gas or propane), injection rate (0.5, 1.5, 3.0, 6.0, 8.0, 10, or 18 MMscfd), and injection pressure (1500, 3000, 5500, or 7500 psi). The target variables for visualization included the following measurements at each of the seven wells (MB1, MB2 (injection well), MB3, TF1, TF2, TF3, and TF4): production (oil, gas, and water production rates and cumulative production), BHP, and tracer (rich gas or propane) production rate and cumulative production.

An online dashboard was created using R-Shiny [41], where users can interactively customize the display. The online dashboard was developed by creating a server that provides the backbone of the visualizations and a user interface (UI) where pages show different time-series visualizations of well performance based on a set of user-defined selections. The interactive function of the input data was accomplished by controllers in R-Shiny, which allow the users to query and extract data from the server. Controllers were created via `CheckboxInput` and/or `RadioButtons` for discrete variables and `SliderInput` for continuous variables. The time-series plots of the well performance variables were created using the R package `ggplot` [42]. The `grid_wrap` function was used so that the data from different wells could be visualized vertically and interactively. The UI has four pages: Welcome, Tracer Injection, Propane Injection, and Prediction. The dashboard is made for operators to view forecasting results conveniently, as illustrated in [Figure 13](#), which shows the tracer (attached to C1) concentration change for Wells MB2, TF2, and TF3 for the given conditions of gas injection rate of 18 MMscfd, closed external offset production wells (MB1, MB3, TF1, and TF4), and 7500-psi injection well BHP.

Forecasting refers to predictive modeling, the rapid generation of a prediction about future performance that the EOR site operator can compare against observed performance. The Prediction page shows visualization of forecasted results from ML-based predictive models that were trained on the reservoir simulations. The created ML models were uploaded to the R-Shiny server and deployed to make predictions of different rich gas EOR scenarios.

## ML Model Development

For this proof of concept, the extreme gradient boosting (XGBoost) algorithm was used for predictive modeling; however, this could be replaced with other ML algorithms. XGBoost is a boosting ensemble learning algorithm that integrates predictions of “weak” tree models to achieve a strong tree model via a sequential process [43]. The simplified XGBoost algorithm works by building a sequential list of decision trees, and in each successive round, the decision tree uses the residuals from the prior tree as the target variable. The loss function, or the errors between the predicted and actual values, are minimized using a gradient descent approach to estimate the coefficients within the XGBoost model. There are seven hyperparameters to tune, and the optimal values were tuned by  $k$ -fold cross-validation ([Table 8](#)).



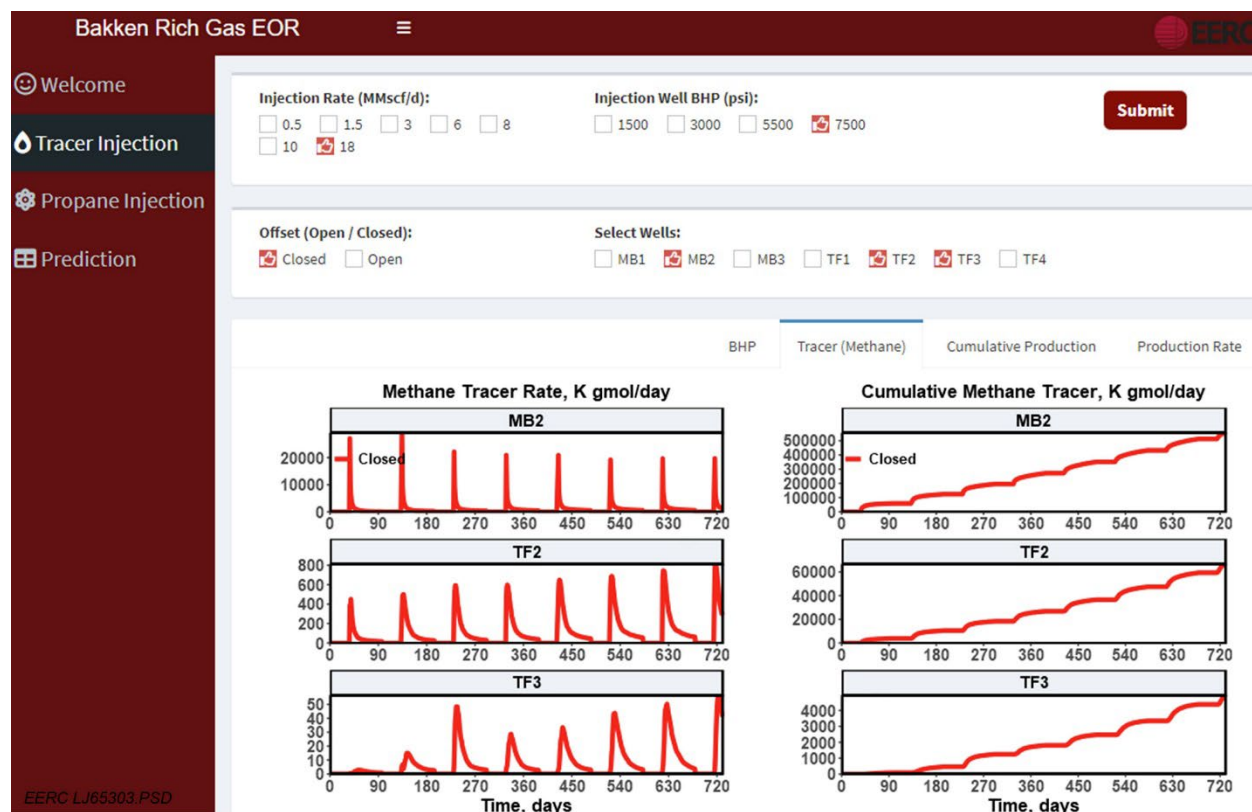


Figure 13. Tracer Injection page of the UI showing the Tracer (attached to C1) tab for Wells MB2, TF2, and TF3 for the given conditions of gas injection rate of 18 MMscfd, closed external offset production wells (MB1, MB3, TF1, and TF4), and 7500-psi injection well BHP.

Table 8. Hyperparameters of the XGBoost Algorithm

Parameter	Description
nrounds	Maximum number of iterations
max_depth	Maximum depth of the tree
gamma	Regularization coefficient
min_child_weight	Minimum number of instances required in a child node
eta	Learning rate
subsample	Number of samples supplied to a tree
colsample_bytree	Number of features (variables) supplied to a tree

The predictor variables were identical to the controllers used in the visualizations: 1) injection rate (0.5, 1.5, 3.0, 6.0, 8.0, 10, or 18 MMscfd), 2) injection well BHP (1500, 3000, 5500, or 7500 psi), and 3) offset well status (open or closed). In addition to these three EOR parameters, the time stamp was also used as an input variable since time is highly correlated with EOR performance. The target variables were oil, water, and gas production rates and cumulative production for the seven wells and two different injectates (rich gas with tracer or propane). Therefore, the total number of target variables was 42: 3 (oil, water, and gas)  $\times$  1 (production rate)  $\times$  7 (seven wells)  $\times$  2 (two injectates). The cumulative production data were calculated from the production rate data, which led to the final number of target variables as 84.

The input data and the 42 target variables (production rate variables) were compiled and used as the data to develop the ML models. The compiled data were randomly divided into training and testing sets by the ratio of 0.8:0.2 (i.e., 80% of the compiled data were randomly placed into the training set, and the remaining 20% were placed into the testing set). The training set was used to train the XGBoost model, and the testing set was used to evaluate the performance of the model. The modeling performance was evaluated using  $r^2$  and relative root mean square error (RRMSE), where a model with high  $r^2$  and low

RRMSE values was considered as a good-performing model. The RRMSE is defined as the value of the root mean square error divided by the mean value of that variable.

Corresponding to the target variables, 84 XGBoost models were developed. The average ( $\pm$  standard deviation) values of  $r^2$  values for both training and testing sets for models with rich gas injection were 0.996 ( $\pm 0.008$ ) and 0.984 ( $\pm 0.025$ ), respectively, and for models with propane injection were 0.997 ( $\pm 0.004$ ) and 0.985 ( $\pm 0.02$ ), respectively. The average ( $\pm$  standard deviation) RRMSE values for both training and testing sets for models with rich gas injection were 0.04 ( $\pm 0.08$ ) and 0.08 ( $\pm 0.16$ ), respectively, and for models with propane injection were 0.03 ( $\pm 0.04$ ) and 0.05 ( $\pm 0.07$ ), respectively.

Figure 14 shows the  $r^2$  and RRMSE performance results for all of the 42 models in the training and testing sets for the models with EOR injection by rich gas or propane. Approximately 60% of the models had  $r^2$  values greater than 0.9, and roughly 85% of the models had RRMSE values less than 0.1 for both training and testing sets. These performance indicators showed that most of the models performed well for both the training and testing sets. Therefore, for the current study, all the models were accepted for predictive modeling purposes.

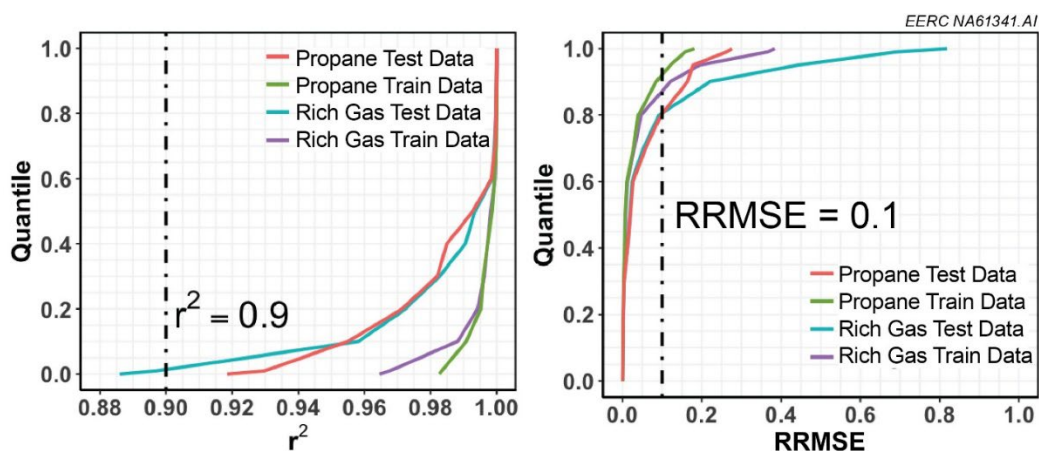


Figure 14. Quantile plots of modeling performance evaluated by  $r^2$  and RRMSE values for the training and testing sets of EOR rich gas or propane injection.

In this proof of concept, the training and testing data for the predictive modeling were the same data as the simulations used for the real-time visualizations. However, this need not be the case. The real-time visualizations are designed to display data acquired in the field and saved to the R-Shiny server; these data can be any data type acquired at various frequencies (e.g., hourly, daily, weekly, etc.). The simulations were used as an example. In contrast, the workflow for developing the predictive models requires reservoir simulations that explore the parameter space of the EOR operating controls. Therefore, prior to initiating the rich gas EOR, it is necessary to have a set of reservoir simulations that identifies the EOR operating controls and their expected ranges, generates the reservoir simulation outputs, and then trains and tests ML-based models using the model development strategy.

Once the XGBoost models were developed, they were saved to a local drive and deployed to the R-Shiny server. The fitted XGBoost models allow the user to create forecasts of the target variables based on their user-defined selections of the predictor variables (injection rate, injection well BHP, and offset well status). These forecasts allow the operator to compare the observed data (visualization) against the forecasted data (prediction) to evaluate whether to continue operating the EOR project as is or to make one or more adjustments.

### Real-Time Control

Control methods refer to operational changes that the EOR site operator can enact (e.g., changing gas injection rates) to affect the observed performance and potentially improve the EOR outcome. The

integration of visualizing reservoir surveillance data in real time, rapidly forecasting reservoir performance, and deploying operational changes to affect EOR performance. The real-time visualizations are designed to show field data for well BHP, tracer or propane breakthrough, production rate, and cumulative production. Real-time forecasting is designed to predict future well performance based on EOR operational controls. In this proof-of-concept study, the EOR operational controls include injection rate, injection well BHP, and offset status (open or closed), as these factors are significantly related to rich gas EOR performance. Comparative assessments between real-time visualization (what is occurring in the field) and forecasting (what is predicted given a set of EOR operational controls) provide a means for real-time control.

## Conclusions

A few EOR pilot tests have been conducted to offset the rapid decline in oil production in single wells of the Bakken Formation since the shale revolution. Most of these pilot tests had gas injection involved; however, only limited research has been reported to investigate actual field implementations and their surveillance for gas EOR in the BPS. A series of activities were performed in this study to explore real-time visualization, forecasting, and control methods for improved reservoir surveillance during EOR processes. The main conclusions can be summarized as follows:

1. Pressure buildup, conformance issues, and timely gas breakthrough detection were some of the main challenges for gas EOR in unconventional wells because of the interconnected fractures between injection and offset wells.
2. Careful EOR design and continuous reservoir monitoring could be key components to mitigate these challenges. Timely gas breakthrough detection followed by immediate control actions through the RSSS system showed effective results in conformance control and pressure buildup.
3. A workflow was developed to explore real-time visualization, forecasting, and control methods for improved reservoir surveillance during EOR processes based on the field pilots and data generated in a large set of synthetic reservoir simulations.
4. ML-based models using the XGBoost algorithm were developed to rapidly forecast well performance given a set of user-defined EOR operating parameters. These predictive models allow the user to modify the offset well status, injection rate, and injection well BHP as well as predict the potential well response during the EOR process.
5. The combination of real-time visualization tools with real-time forecasting tools provides a framework for real-time control—operational changes that the EOR site operator can enact (e.g., changing gas injection rates) to affect the observed performance and potentially improve the EOR outcome.

## Acknowledgments

This work was supported by the U.S. Department of Energy (DOE) through Cooperative Agreement No. DE-FE0024233, and the Bakken Production Optimization Program at the Energy & Environmental Research Center. This manuscript was developed from Subactivity 8.2.1 – Real-Time Visualization, Forecasting, and Control of the project report to DOE [28]. The authors appreciate the data and financial support provided by partner organizations. The simulation work conducted under this program was made possible by contributions of software licenses from CMG, SimTech, and SLB.

## References

1. Sorensen JA, Kurz BA, Hawthorne SB, Jin L, Smith SA, Azenkeng A. Laboratory characterization and modeling to examine CO<sub>2</sub> storage and enhanced oil recovery in an unconventional tight oil formation. *Energy Procedia*. 2017 Jul 1;114:5460–78.
2. Jin L, Sorensen JA, Hawthorne SB, Smith SA, Pekot LJ, Bosshart NW, Burton-Kelly ME, Miller DJ, Grabanski CB, Gorecki CD, Steadman EN. Improving oil recovery by use of carbon dioxide in the Bakken unconventional system: A laboratory investigation. *SPE Reservoir Evaluation & Engineering*. 2017 Aug 1;20(03):602–12.
3. Jin L, Hawthorne S, Sorensen J, Pekot L, Kurz B, Smith S, Heebink L, Herdegen V, Bosshart N, Torres J, Dalkhaa C, Peterson K, Gorecki C, Steadman E, Harju J. Advancing CO<sub>2</sub> enhanced oil recovery and storage in unconventional oil play—Experimental studies on Bakken shales. *Applied Energy*. 2017 Dec 15;208:171–83.
4. Hawthorne SB, Miller DJ, Grabanski CB, Jin L. Experimental Determinations of Minimum Miscibility Pressures Using Hydrocarbon Gases and CO<sub>2</sub> for Crude Oils from the Bakken and Cut Bank Oil Reservoirs. *Energy & Fuels*. 2020 Apr 20;34(5):6148–57.
5. Hawthorne SB, Grabanski CB, Jin L, Bosshart NW, Miller DJ. Comparison of CO<sub>2</sub> and Produced Gas Hydrocarbons to Recover Crude Oil from Williston Basin Shale and Mudrock Cores at 10.3, 17.2, and 34.5 MPa and 110° C. *Energy & Fuels*. 2021 Mar 31;35(8):6658–72.
6. Wan, X., Jin, L., Azzolina, N.A., Butler, S.K., Yu, X., Zhao, J., 2022, Applying Reservoir Simulation and Artificial Intelligence Algorithms to Optimize Fracture Characterization and CO<sub>2</sub> Enhanced Oil Recovery in Unconventional Reservoirs: A Case Study in the Wolfcamp Formation. *Energies* 2022, 15, 8266.
7. Wan, X., Jin, L., Azzolina, N.A., Zhao, J., Yu, X., Smith, S.A. and Sorensen, J.A., 2023. Optimization of operational strategies for rich gas enhanced oil recovery based on a pilot test in the Bakken tight oil reservoir. *Petroleum Science*.
8. Kazempour, M., Kiani, M., Nguyen, D., Salehi, M., Bidhendi, M.M., and Lantz, M., 2018, Boosting oil recovery in unconventional resources utilizing wettability altering agents— successful translation from laboratory to field: Presented at the SPE Improved Oil Recovery Conference, Tulsa, Oklahoma.
9. Hoffman, T.B., and Evans, J.G., 2016, Improved oil recovery IOR pilot projects in the Bakken Formation: Presented at the SPE Low Perm Symposium, Denver, Colorado.
10. Sorensen, J.A., Pekot, L.J., Torres, J.A., Jin, L., Hawthorne, S.B., Smith, S.A., Jacobson, L.L., and Doll, T.E., 2018, Field test of CO<sub>2</sub> injection in a vertical Middle Bakken well to evaluate the potential for enhanced oil recovery and CO<sub>2</sub> storage: Paper presented at the Unconventional Resources Technology Conference, Houston, Texas, July 23–25, 2018, URTeC Paper No. 2902813.
11. Pospisil, G., Weddle, P., Strickland, S., McChesney, J., Tompkins, K., Neuroth, T., Pearson, C.M., Griffin, L., Kaier, T., Sorensen, J. and Jin, L., 2020, October. Report on the first rich gas EOR cyclic multiwell huff n puff pilot in the bakken tight oil play. In SPE Annual Technical Conference and Exhibition? (p. D041S051R002).
12. Pospisil, G., Griffin, L., Souther, T., Strickland, S., McChesney, J., Pearson, C.M., Dalkhaa, C., Sorensen, J., Hamling, J., Kurz, B. and Bosshart, N., 2022, October. East Nesson Bakken enhanced oil recovery pilot: Coinjection of produced gas and a water-surfactant mixture. In Unconventional Resources Technology Conference, 20–22 June 2022 (pp. 803–823).
13. Rivero JT, Jin L, Bosshart N, Pekot LJ, Sorensen JA, Peterson K, Anderson P, Hawthorne SB. Multiscale Modeling to Evaluate the Mechanisms Controlling CO<sub>2</sub>-Based Enhanced Oil Recovery and CO<sub>2</sub> Storage in the Bakken Formation. In SPE/AAPG/SEG Unconventional Resources Technology Conference 2018 Jul 23.
14. Nagarajan, N.R., Stoll, D., Litvak, M.L., Prasad, R.S., and Shaarawi, K., 2020, Successful field test of enhancing Bakken oil recovery by propane injection Part I. field test planning, operations, surveillance, and results: Presented at the SPE/AAPG/SEG Unconventional Resources Technology Conference, virtual: URTEC-2020-2768-MS.

15. Litvak, M.L., Nagarajan, N.R., Prasad, R.S. and Shaarawi, K., 2020, December. Successful field test of enhancing Bakken oil recovery with propane injection Part II. development and application of innovative simulation technology. In Unconventional Resources Technology Conference, 20–22 July 2020.
16. Zhao, J., Jin, L., Azzolina, N.A., Wan, X., Yu, X., Sorensen, J.A., Kurz, B.A., Bosshart, N.W., Smith, S.A., Wu, C. and Vrtis, J.L., 2022. Investigating enhanced oil recovery in unconventional reservoirs based on field case review, laboratory, and simulation studies. *Energy & Fuels*, 36(24), pp.14771–14788.
17. Yuncong, G.A., Mifu, Z.H., Jianbo, W.A., and Chang, Z.O., 2014, Performance and gas breakthrough during CO<sub>2</sub> immiscible flooding in ultra-low permeability reservoirs: *Petroleum Exploration and Development*, v. 41, p. 88–95.
18. Rassenfoss, S., 2024. Chevron Applies Some Unconventional Thinking To Try To Make Shale EOR a Standard Treatment. *Journal of Petroleum Technology*, 76(02), pp.24–28.
19. Zhang, L., Huang, H., Wang, Y., Ren, B., Ren, S., Chen, G., and Zhang, H., 2014, CO<sub>2</sub> storage safety and leakage monitoring in the CCS demonstration project of Jilin oilfield, China: *Greenhouse Gases: Science and Technology*, v. 4, p. 425–439.
20. Alfi, M., Hosseini, S.A., Alfi, M., and Shakiba, M., 2015, Effectiveness of 4D seismic data to monitor CO<sub>2</sub> plume in Cranfield CO<sub>2</sub>-EOR project: Presented at the Carbon Management Technology Conference, November 17.
21. Jervis, M., Bakulin, A., and Smith, R., 2018, Making time-lapse seismic work in a complex desert environment for CO<sub>2</sub> EOR monitoring—design and acquisition: *The Leading Edge*, v. 37, no. 8, p. 598–606.
22. Zaluski, W., El-Kaseeh, G., Lee, S.Y., Piercey, M., and Duguid, A., 2016, Monitoring technology ranking methodology for CO<sub>2</sub>-EOR sites using the Weyburn-Midale Field as a case study: *International Journal of Greenhouse Gas Control*, v. 54, p. 466–478.
23. Jin, L., Barajas-Olalde, C., Bosshart, N., He, J., Adams, D., Kalenze, N., Hamling, J., and Gorecki, C., 2021, Application of CO<sub>2</sub> injection monitoring techniques for CO<sub>2</sub> EOR and associated geologic storage: Available at SSRN 3812730, March 25.
24. Mur, A., Barajas-Olalde, C., Adams, D.C., Jin, L., He, J., Hamling, J.A., and Gorecki, C.D., 2020, Integrated simulation to seismic and seismic reservoir characterization in a CO<sub>2</sub> EOR monitoring application: *The Leading Edge*, v. 39, no. 9, p. 668–78.
25. Salako, O., Jin, L., Barajas-Olalde, C., Hamling, J. A., & Gorecki, C. D. Implementing adaptive scaling and dynamic well-tie for quantitative 4-D seismic evaluation of a reservoir subjected to CO<sub>2</sub> enhanced oil recovery and associated storage. *International Journal of Greenhouse Gas Control*, 2018:78:306-326.
26. Barajas-Olalde C, Haffinger P, Gisolf D, Zhang M, Droujinina A, Doulgieris P, Khatibi S, Jin L, Burnison SA, Hamling JA, Gorecki CD. Simultaneous time-lapse WEB-AVO inversion for seismic reservoir monitoring: Application to CO<sub>2</sub> enhanced oil recovery at the Bell Creek oil field. In SEG Technical Program Expanded Abstracts, 2019 Aug 10 (pp. 564–568). Society of Exploration Geophysicists.
27. Barajas-Olalde, C., Mur, A., Adams, D.C., Jin, L., He, J., Hamling, J.A. and Gorecki, C.D., 2021. Joint impedance and facies inversion of time-lapse seismic data for improving monitoring of CO<sub>2</sub> incidentally stored from CO<sub>2</sub> EOR. *International Journal of Greenhouse Gas Control*, 112, p.103501.
28. Smith, S.A., Sorensen, J.A., Kurz, B.A., Heebink, L.V., Azzolina, N.A., Jin, L., Kong, L., Yu, X., Wan, X., Yu, Y., Zhao, J., Beddoe, C.J., Mibeck, B.A.F., Butler, S.K., Azenkeng, A., Kurz, M.D., Wocken, C.A., Chakhmakhchev, A.V., Jiang, T., Bosshart, N.W., Burton-Kelly, M.E., Nakles, D.V., Gorecki, C.D., Harju, J.A., and Steadman, E.N., 2022. Findings on Subtask 3.1-Bakken Rich Gas Enhanced Oil Recovery Project (No. DE-FE0024233). *Energy & Environmental Research Center University of North Dakota*.

29. Kumar, A., and Sharma, M.M., 2018, Diagnosing fracture-wellbore connectivity using chemical tracer flowback data: Presented at the SPE/AAPG/SEG Unconventional Resources Technology Conference, July 23.
30. Tayyib, D., Al-Qasim, A., Kokal, S., and Huseby, O., 2019, Overview of tracer applications in oil and gas industry: Paper presented at the SPE Kuwait Oil & Gas Show and Conference, Mishref, Kuwait, October.
31. Al-Qasim, A., Kokal, S., Hartvig, S., and Huseby, O., 2019, Reservoir description insights from inter-well gas tracer test: Presented at the Abu Dhabi International Petroleum Exhibition & Conference, November 11.
32. Al-Qasim, A., Kokal, S., Hartvig, S., and Huseby O., 2020, Subsurface monitoring and surveillance using inter-well gas tracers: *Upstream Oil and Gas Technology*, v. 3. 100006.
33. Sharma, A., Shook, G.M., and Pope, G.A., 2014, Rapid analysis of tracers for use in EOR flood optimization: Presented at the SPE Improved Oil Recovery Symposium, April 12.
34. Sanni, M., Abbad, M., Kokal, S., Ali, R., Zefzafy, I., Hartvig, S., and Huseby, O., 2017, A field case study of an interwell gas tracer test for gas-EOR monitoring: Presented at the Abu Dhabi International Petroleum Exhibition & Conference, November 13.
35. Huseby, O., Sagen, J., Wangen, M., and Viig, S.O., 2010, Planning and interpretation of offshore-field tracer tests using accurate and refined tracer simulations: Presented at the SPE Latin American and Caribbean Petroleum Engineering Conference, December 1.
36. Al-Abbad, M.A., Sanni, M.L., Kokal, S., Krivokapic, A., Dye, C., Dugstad, Ø., Hartvig, S.K., and Huseby, O.K., 2019, A step change for single-well chemical-tracer tests: field pilot testing of new sets of novel tracers: *SPE Reservoir Evaluation & Engineering*, 2019, v. 22, no. 1, p. 253–265.
37. Chen, H., Chang, S., Thomas, G., Wang, W., Mashat, A., and Shateeb, H., 2021, Comparison of water and gas tracers field breakthrough: Presented at the SPE Annual Technical Conference and Exhibition, September 15.
38. North Dakota Industrial Commission (NDIC), 2024. [www.dmr.nd.gov/oilgas/](http://www.dmr.nd.gov/oilgas/). Accessed on March 25, 2024.
39. Jin, L., Kurz, B.A., Ardali, M., Wan, X., Zhao, J., He, J., Hawthorne, S.B., Djezzar, A.B., Yu, Y., Morris, D. 2022. Investigation of Produced Gas Injection in the Bakken for Enhanced Oil Recovery Considering Well Interference. URTeC-3723697. Proceedings of Unconventional Resources Technology Conference (URTeC), Houston, Texas, USA, 20–22 June 2022.
40. Jin, L., Wan, X., Azzolina, N.A., Bosshart, N.W., Zhao, J., Yu, Y., Yu, X., Smith, S.A., Sorensen, J.A., Gorecki, C.D. 2022. Optimizing Conformance Control for Gas Injection EOR in Unconventional Reservoirs. *Fuel* 324 (2022) 124523.
41. Chang, W., Cheng, J., Allaire, J.J., Sievert, C., Schloerke, B., Xie, Y., Allen, J., McPherson, J., Dipert, A., and Borges, B., 2021, Shiny: Web Application Framework for R. R package version 1.6.0. <https://CRAN.R-project.org/package=shiny> (accessed 2021).
42. Wickham, H., 2016, *ggplot2: Elegant Graphics for Data Analysis*. Springer-Verlag New York, 2016.
43. Chen, T., and Guestrin, C., 2016, XGBoost—a scalable tree boosting system, in *Proceedings of the 22nd ACM SIGKDD International Conference on Knowledge Discovery and Data Mining*: New York, New York, p. 785–794.